

Path integral derivation of the thermofield double state in causal diamonds

Abhijit Chakraborty,^a Carlos R. Ordóñez^b and Gustavo Valdivia-Mera^b

^a*Institute for Quantum Computing, University of Waterloo,
Waterloo, ON, N2L 3G1, Canada*

^b*Department of Physics, University of Houston
Houston, Texas 77204-5005, USA*

E-mail: abhijit.chakraborty@uwaterloo.ca, cordonez@central.uh.edu,
gvaldiviamera@uh.edu

ABSTRACT: In this article, we follow the framework given in the article *Physica A*, **158**, pg 58-63 (1989) by R. Laflamme to derive the thermofield double state for a causal diamond using the Euclidean path integral formalism, and subsequently derive the causal diamond temperature. The interpretation of the physical and fictitious system in the thermofield double state arises naturally from the boundary conditions of the fields defined on the Euclidean sections of the cylindrical background geometry $S_\beta^1 \times \mathbb{R}$, where β defines the periodicity of the Euclidean time coordinate and S_β^1 is the one-dimensional sphere (circle). The temperature detected by a static diamond observer at $x = 0$ matches with the thermofield double temperature derived via this path integral procedure.

Contents

1	Introduction	1
2	Brief review of the geometric interpretation of a TFD state	3
2.1	Euclidean Formalism	3
2.2	The cylinder	3
3	Thermofield Double State in Causal Diamonds	4
3.1	Massless scalar field	5
3.2	Massive scalar field	6
3.3	Thermofield Double State	7
4	Density matrix and Diamond Temperature	9
5	Conclusions	10
A	Computation of the Euclidean Action	11
A.1	Massless field	11
A.2	Massive field	12

1 Introduction

Stephen Hawking, in his seminal work in 1975, showed that black holes can emit thermal radiation if one considers quantum effects [1]. Hawking’s results [1–3] were subsequently corroborated by a series of papers by Unruh, Fulling, Davies, Parker, and Wald [4–10], which flourished into a new field of research on quantum effects in curved spacetime.

Around the same time, Umezawa and Takahashi, motivated by studies in many-body physics, developed the thermofield dynamics formalism, in which they constructed a temperature-dependent vacuum state denoted as $|0(\beta)\rangle$, the thermofield double state (TFD) [11–14]. The purpose of this state was to meet the requirement that the vacuum expectation value for any observable would be numerically equal to the statistical average obtained for an ensemble in thermal equilibrium. In other words, $\langle 0(\beta) | F | 0(\beta) \rangle = Z^{-1}(\beta) \sum_n e^{-\beta E_n} \langle n | F | n \rangle$, where F represents an observable, E_n are energy eigenvalues, and $Z(\beta)$ is the partition function. To accomplish this goal, they introduced a fictitious dynamical system mirroring the original system. Through this approach, they showed that the ‘thermal’ vacuum state fulfilling the desired condition can be expressed as $|0(\beta)\rangle = Z^{-1/2}(\beta) \sum_n e^{-\beta E_n/2} |n, \tilde{n}\rangle$, where $|\tilde{n}\rangle$ is the energy eigenstate of the field defined on the fictitious system.

Shortly after Umezawa and Takahashi's introduction of thermofield dynamics, Israel showed that one can interpret the vacuum state for a scalar field theory defined on extensions of Schwarzschild and Rindler spacetimes – Kruskal and Minkowski, respectively – as the Umezawa-Takahashi's thermofield double state (TFD) [15]. Time-reversed copies of Rindler and Schwarzschild geometries can be identified within these extended spacetimes. It is precisely on these copies that the fictitious fields are defined. Since an observer restricted in the Rindler and Schwarzschild spacetime will only have access to the original system, the degrees of freedom of the fictitious system need to be averaged over, which gives rise to the thermal behavior of the Minkowski or Kruskal vacuum. In other words, the emergence of the thermal behavior in the TFD takes place when the observation of particle modes is restricted due to the presence of horizons. The temperature of the TFD state is usually determined by the intrinsic parameters of the system, such as surface gravity or acceleration in the Schwarzschild and Rindler case, respectively.

In a series of beautiful papers, Laflamme later showed that the TFD can be obtained through the path integral approach [16, 17]. In this context, the field's boundary conditions are set on Euclidean sections obtained by unwrapping the original manifold, where the identification of imaginary time $\tau \sim \tau + \beta$ takes place. This identification, typically associated with the periodicity of the polar plane, $\theta \sim \theta + 2\pi$, is necessary to avoid conical singularities and maintain the smoothness of the geometry. Additionally, the periodicity β holds a deeper significance as it bridges the gap between geometry and thermodynamics. When working within Euclidean sections and developing the field theory, we find that this value precisely corresponds to the inverse of the temperature of the ensemble described by the TFD.

Our goal in this article is to apply the elegant methodology developed by Laflamme to the causal diamond (CD) [18, 19]. Unlike the Unruh-Davis effect, in this case, the observers remain stationary at the origin. However, they are subjected to a finite lifetime. This condition gives rise to past and future horizons defining the CD. As Israel noted, the presence of these horizons generates a thermal spectrum. This is due to the limited access to particle modes, causing the physical system to manifest as a mixed quantum state. Causal diamonds provide an interesting insight into the Unruh-like radiation phenomenon because they highlight the sole role of the horizon in thermality in the absence of acceleration. The thermal effect also has a better chance of being detected in tabletop experiments due to the fact that measuring the effect does not require means to create an absurdly high acceleration. Due to these reasons, and its close connection to both black hole physics and quantum many-body theory, causal diamonds have seen a recent upsurge of interest in the community [20–30].

Our article is organized in the following way. In section II, we provide a brief summary of the framework used by Laflamme to set up our calculations. In section III, we analyze the Euclidean action of the CD and, through suitable transformations, we adapt it into a recognizable form for subsequent calculations, leading us to the TFD. We investigate both

massless and massive cases. In section IV, we compute the density matrix of the original physical system and demonstrate that the initially imposed geometric conditions allow us to calculate the equilibrium temperature of the thermal bath in a few steps. Finally, we conclude with a discussion on this framework in section V.

2 Brief review of the geometric interpretation of a TFD state

In this section, we provide a brief overview of the method used by Laflamme in refs. [16, 17] to elucidate the connection between geometry and the thermofield double structure of the vacuum state.

2.1 Euclidean Formalism

The Euclidean path integral, $\int D\Phi e^{-S_E[\Phi]}$, where $S_E[\Phi]$ denotes the Euclidean action, gives us the probability amplitude between two field states, such that the probability density is given by $e^{-S_E[\Phi]}$. Similarly, the probability amplitude when the field possesses a property A is given by

$$P(A) = \int D\Phi \Pi(A) e^{-S_E}. \quad (2.1)$$

Here, $\Pi(A)$ is equal to 1 if the field possesses the given property and zero otherwise. Property A denotes the existence of a surface S that divides the manifold M into two equal parts, M_{\pm} , such that the field has the value Φ on that surface. In addition, since both submanifolds M_{\pm} share this property, $P(A)$ will have contributions from S_E on both submanifolds. In other words,

$$P(A) = \int_{M_+} D\Phi e^{-S_E[\Phi]} \int_{M_-} D\Phi e^{-S_E[\Phi]}. \quad (2.2)$$

2.2 The cylinder

Let us consider the manifold M to be the cylinder given by $S^1_{\beta} \times \mathbb{R}$ (figure 1a), which is obtained by identifying the time coordinate in such a way that it acquires a periodicity of β . Subsequently, through two consecutive cuts along the foliations $t_E = \tau_1$ and $t_E = \tau_2$, we can unroll the cylinder and divide the plane into two equal parts ($\tau_2 = \tau_1 + \beta/2$). See figure 1b.

Let us denote these submanifolds as M_{\pm} . Thus, from the property mentioned in section 2.1, we define the field to be $\Phi = \Phi_1$ at τ_1 and $\Phi = \Phi_2$ at τ_2 . Then, the Euclidean path integrals on each submanifold are

$$K_+[\Phi_1, \Phi_2] = \int_{\Phi_1}^{\Phi_2} D\Phi e^{-S_E[\Phi]}, \quad K_-[\Phi_1, \Phi_2] = \int_{\Phi_2}^{\Phi_1} D\Phi e^{-S_E[\Phi]}. \quad (2.3)$$

It is essential to mention that this geometric structure is of great significance since the periodicity in t_E is closely related to the smoothness condition of the manifold in the polar plane, (θ, r) . We know that unless θ has a periodicity of 2π , the manifold will exhibit a conical-type singularity. Furthermore, in the Euclidean quantum field theory, the value of

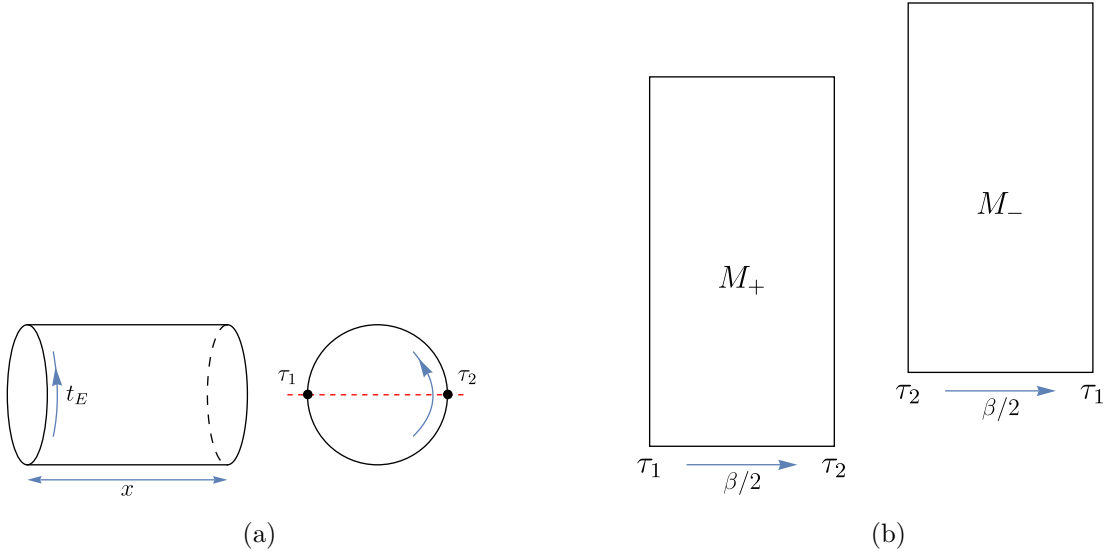


Figure 1: (a) Left: Manifold M defined by $S^1_\beta \times \mathbb{R}$ with periodicity along the Euclidean time coordinate. Right: Cross-section of the manifold M . (b) Manifolds M_+ and M_- , obtained through two successive cuts along τ_1 and τ_2 .

β corresponds to the inverse of the temperature of the thermal bath that characterizes the vacuum state of the field. This will be precisely utilized to calculate the temperature of the causal diamond in section 4.

3 Thermofield Double State in Causal Diamonds

Let us analyze a real scalar field $\phi(x)$ on the 2-dimensional background geometry provided by the causal diamond. Then, the Euclidean action is

$$S_E = \frac{1}{2} \int \sqrt{g} d^2x [g^{\mu\nu} \partial_\mu \phi \partial_\nu \phi + m^2 \phi]. \quad (3.1)$$

The causal diamond is the spacetime region defined by the intersection of the past light cone corresponding to the death event, and the future light cone corresponding to the birth event of an observer with a finite lifetime given by 2α (figure 2a). In this section, we are utilizing the coordinate transformation defined by the map given by the composition of a special conformal transformation and a spatial translation (see ref. [31]),

$$(t_d, x_d) = T(-\alpha) \circ K\left(\frac{1}{2\alpha}\right)(t_r, x_r). \quad (3.2)$$

where

$$K(\rho) x^\mu = \frac{x^\mu + \delta_1^\mu \rho x^2}{1 + 2\rho x^1 + \rho^2 x^2}, \quad T(a) x^\mu = (x^0, x^1 + a). \quad (3.3)$$

Here, (t_d, x_d) are the points in Minkowski spacetime restricted to the interior of the causal diamond (figure 2c), and (t_r, x_r) are those restricted to the right Rindler wedge

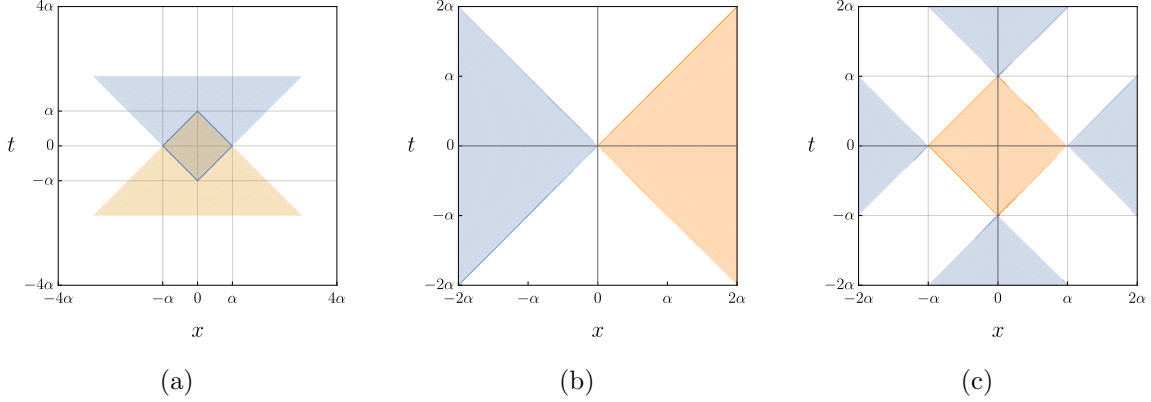


Figure 2: (a) Causal diamond formed by the intersection of the light cone corresponding to birth and death events for an observer with a lifetime of 2α . (b) Left and right Rindler wedges. (c) Interior and exterior regions of the causal diamond.

(figure 2b). $K(\rho)$ represents a special conformal transformation, whose effect is to compactify the unbounded right Rindler wedge into a diamond of size ρ^{-1} while keeping the causal structure unchanged. The spatial transformation is denoted by $T(a)$, which laterally shifts the diamond to the origin by an amount a . δ_λ^μ is the Kronecker delta function and the superscript 1 denotes the spatial component. Let us use the following coordinate transformation between Minkowski and Rindler, in which $\xi > 0$ and $-\infty < \tau < \infty$,

$$t_r = \xi \sinh(\tau/\alpha), \quad x_r = \xi \cosh(\tau/\alpha). \quad (3.4)$$

Furthermore, it is important to note that the mapping between the left Rindler wedge and the external region of the causal diamond (blue-colored regions in figures 2b and 2c) is obtained by changing $t_r \rightarrow -t_r$ and $x_r \rightarrow -x_r$ in equation (3.4).

In Euclidean signature, obtained by $\tau \rightarrow -i\tau$ (and considering from now on τ as Euclidean coordinate), the line element for the causal diamond is conformal to Rindler,

$$ds^2 = \Omega^2(\tau, \xi) \left[\frac{\xi^2}{\alpha^2} d\tau^2 + d\xi^2 \right], \quad (3.5)$$

where the conformal factor is given by

$$\Omega^2(\tau, \xi) = \frac{16\alpha^4}{(4\alpha\xi \cos(\frac{\tau}{\alpha}) + \xi^2 + 4\alpha^2)^2}. \quad (3.6)$$

Thus, the Euclidean action (3.1) takes the following form

$$S_E = -\frac{1}{2} \int d\xi d\tau \phi \left[\frac{\alpha}{\xi} \partial_\tau^2 + \frac{1}{\alpha} \partial_\xi + \frac{\xi}{\alpha} \partial_\xi^2 - m^2 \frac{\Omega^2 \xi}{\alpha} \right] \phi. \quad (3.7)$$

3.1 Massless scalar field

Let us set $m = 0$ and $\xi = \alpha e^{\rho/\alpha}$ in the Euclidean action (3.7). Thus, we obtain

$$S_E = -\frac{1}{2} \int d\rho d\tau \phi [\partial_\tau^2 + \partial_\rho^2] \phi. \quad (3.8)$$

From the Fourier transformation of the scalar field, we obtain the following form of the Euclidean action (see appendix A.1 for details)

$$S_E = -\frac{1}{2} \int d\tau \int \frac{d\lambda}{2\pi} \phi(\tau, \lambda) \partial_\tau^2 \phi^*(\tau, \lambda) + \frac{1}{2} \int d\tau \int \frac{d\lambda}{2\pi} \phi(\tau, \lambda) \lambda^2 \phi^*(\tau, \lambda). \quad (3.9)$$

It is noteworthy that, from the separability of the field as defined by $\phi(\tau, \lambda) = \sqrt{2\pi} \psi(\tau) \chi(\lambda)$, we obtain

$$S_E = -\frac{1}{2} \int d\tau \psi(\tau) \partial_\tau^2 \psi(\tau) \int d\lambda \chi(\lambda)^2 + \frac{1}{2} \int d\tau \psi(\tau)^2 \int d\lambda \lambda^2 \chi(\lambda)^2. \quad (3.10)$$

By discretizing the integrals in λ , we can describe the action for each mode. In this way, we obtain the harmonic oscillator action for each single mode λ ,

$$S_E = -\frac{1}{2} \int d\tau \psi_\lambda(\tau) [\partial_\tau^2 - \lambda^2] \psi_\lambda(\tau). \quad (3.11)$$

From Laflamme's method, we identify the manifold on which the action (3.11) is defined as M_+ , thereby establishing $\beta/2 = \tau_2 - \tau_1$. Furthermore, being quadratic in the field, the Euclidean path integral $K_+[\psi_1, \psi_2]$ can be precisely computed.

$$K_+[\psi_1, \psi_2] = \left(\frac{\lambda}{2\pi \sinh\left(\frac{\lambda\beta}{2}\right)} \right)^{1/2} \exp \left[-\frac{\lambda}{2} \left((\psi_1^2 + \psi_2^2) \coth\left(\frac{\lambda\beta}{2}\right) - \frac{2\psi_1\psi_2}{\sinh\left(\frac{\lambda\beta}{2}\right)} \right) \right]. \quad (3.12)$$

The above result can be reformulated in terms of the n -excited state of the Harmonic Oscillator, utilizing Hermite polynomials $H_n(x)$,

$$K_+[\psi_1, \psi_2] = \frac{1}{\sqrt{Z(\beta)}} \sum_{n=0}^{\infty} e^{-\frac{\beta}{2} E_n} \varphi_n(\psi_1) \varphi_n(\psi_2), \quad (3.13)$$

$$\varphi_n(\psi) = \left(\sqrt{\frac{\lambda}{\pi}} \frac{1}{2^n n!} \right)^{1/2} H_n(\sqrt{\lambda}\psi) e^{-\frac{\lambda}{2}\psi^2}, \quad (3.14)$$

where $E_n = \hbar\lambda(n + 1/2)$. In addition, the normalization factor Z depends on β ,

$$1 = \int_{-\infty}^{\infty} d\psi_1 d\psi_2 K_+[\psi_1, \psi_2] K_-[\psi_1, \psi_2] = \frac{1}{Z} \sum_{n=0}^{\infty} e^{-\beta E_n}. \quad (3.15)$$

3.2 Massive scalar field

By expanding the conformal factor (3.6) in powers of ξ , we notice that it can be written as

$$\Omega^2(\tau, \xi) = 1 + \sum_{n=1} \xi^n f_n(\tau). \quad (3.16)$$

Thus, using (3.16) and $A_\xi = \xi \partial_\xi + \xi^2 \partial_\xi^2 - m^2 \xi^2$ in the action (3.7) we obtain

$$S_E = -\frac{1}{2} \int d\xi d\tau \phi \left[\frac{\alpha}{\xi} \partial_\tau^2 + \frac{1}{\alpha \xi} A_\xi \right] \phi + \frac{m^2}{2\alpha} \int d\xi d\tau \phi \left[\sum_{n=1} \xi^{n+1} f_n(\tau) \right] \phi. \quad (3.17)$$

Let us consider the action of the operator A_ξ on the scalar field, given by $A_\xi\phi(\tau, \xi) = -\lambda\phi(\tau, \xi)$. This expression implies the separability of the field, characterised by $\phi(\tau, \xi) = \psi(\tau)\zeta(\xi)/\sqrt{\alpha}$. Therefore, $\zeta(\xi)$ is defined in terms of the modified Bessel function of the second kind $K_{i\sqrt{\lambda}}(m\xi)$, for which the differential equation $A_\xi K_{i\sqrt{\lambda}}(m\xi) = -\lambda K_{i\sqrt{\lambda}}(m\xi)$ is satisfied. Moreover, from the Kontorovich–Lebedev transformation [32, 33], we have

$$\zeta(\xi) = \frac{1}{\pi^2} \int_0^\infty d\lambda \zeta(\lambda) K_{i\sqrt{\lambda}}(m\xi) \sinh(\pi\sqrt{\lambda}), \quad (3.18)$$

$$\zeta(\lambda) = \int_0^\infty d\xi \frac{\zeta(\xi)}{\xi} K_{i\sqrt{\lambda}}(m\xi). \quad (3.19)$$

Thus, the Euclidean action is given by

$$\begin{aligned} S_E = & -\frac{1}{2} \int d\tau \psi(\tau) \partial_\tau^2 \psi(\tau) \int \frac{d\xi}{\xi} \zeta(\xi)^2 - \frac{1}{2\alpha^2} \int d\tau \psi(\tau)^2 \int \frac{d\xi}{\xi} \zeta(\xi) A_\xi \zeta(\xi) \\ & + \sum_{n=1} \int d\tau f_n(\tau) \psi(\tau)^2 \int d\xi \frac{m^2}{2\alpha^2} \xi^{n+1} \zeta(\xi)^2. \end{aligned} \quad (3.20)$$

Using transformations (3.18), we can observe that the integral with respect to ξ in the third term is proportional to m^{-n} . Thus, for large m , we can neglect its contribution to the action. Furthermore, the integrals with respect to ξ in the first and second term of (3.20) can be expressed in terms of λ through the transformations (3.18) and (3.19) (see appendix A.2 for details),

$$\begin{aligned} S_E = & -\frac{1}{2} \int d\tau \psi(\tau) \partial_\tau^2 \psi(\tau) \int \frac{d\lambda}{\pi^2} \zeta(\lambda)^2 \sinh(\pi\sqrt{\lambda}) \\ & + \frac{1}{2\alpha^2} \int d\tau \psi(\tau)^2 \int \frac{d\lambda}{\pi^2} \lambda \zeta(\lambda)^2 \sinh(\pi\sqrt{\lambda}). \end{aligned} \quad (3.21)$$

Furthermore, discretizing the integrals with respect to λ enables us to establish the action for each mode λ ,

$$S_E = -\frac{1}{2} \int d\tau \psi_\lambda(\tau) [\partial_\tau^2 - \omega_\lambda^2] \psi_\lambda(\tau). \quad (3.22)$$

Therefore, the action takes the form of a harmonic oscillator, for each mode λ , as we observed in the massless case. In this way, the Euclidean path integral is again given by (3.13), with $\lambda \rightarrow \omega_\lambda$ in (3.12).

3.3 Thermofield Double State

To identify the fields ψ_1 and ψ_2 in (3.13) within the context of the causal diamond, we first revisit the analysis conducted in Rindler spacetime.

In Rindler coordinates, given by the transformation (3.4), the metric is independent of τ ,

$$ds^2 = -\frac{\xi^2}{\alpha^2} d\tau^2 + d\xi^2. \quad (3.23)$$

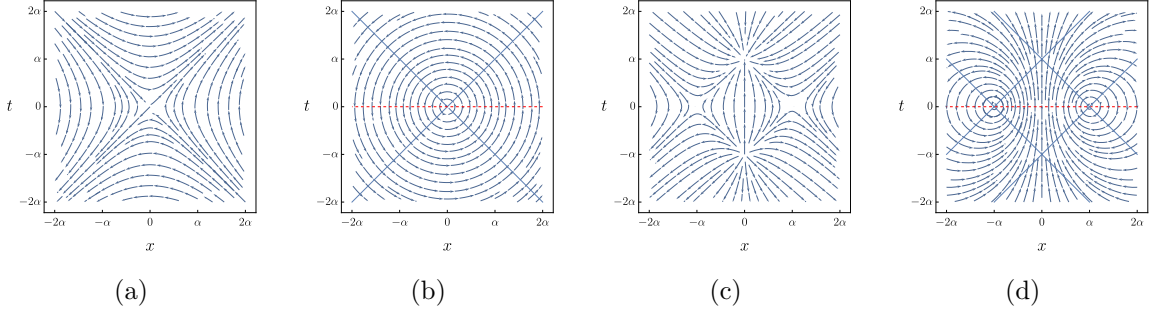


Figure 3: Vector field ∂_τ for Rindler in Lorentzian (a) and Euclidean signature (b), and Causal Diamond in Lorentzian (c) and Euclidean signature (d).

Therefore, the killing vector associated with this symmetry, both in the right and left wedges, is the generator of time evolution. Expressing it in Minkowski coordinates, we have

$$\partial_\tau = \frac{\partial x}{\partial \tau} \partial_x + \frac{\partial t}{\partial \tau} \partial_t = \frac{1}{\alpha} (t \partial_x + x \partial_t). \quad (3.24)$$

Note that the generator of time evolution in Rindler corresponds to the boost generator in the x direction of Minkowski. The integral curves of this vector field are shown in figure 3a, where we observe forward time evolution in the right wedge and backward time evolution in the left wedge. However, in Euclidean signature ($\tau \rightarrow -i\tau$), the vector field (3.24) becomes the generator of counterclockwise rotations in the Euclidean plane (see figure 3b),

$$\partial_\tau = \frac{1}{\alpha} (-t_E \partial_x + x \partial_{t_E}). \quad (3.25)$$

This result is crucial as it provides a better understanding of the Euclidean path integral and the role of the cylinder in Laflamme's proposal. As mentioned in the paragraph after equation (3.11), we identify the manifold over which the action is defined as M_+ . Therefore, the evolution from τ_1 to τ_2 , precisely half the periodicity β , is interpreted as the propagation of Rindler fields, observed in the Euclidean plane, involving a rotation of π radians. In other words, the evolution occurs from states defined in the left (at $\theta = -\pi$) wedge to those in the right (at $\theta = 0$). This is precisely where we observe the connection between the cylinder defined by Laflamme (figure 1a) and the propagation of states from the left wedge to the right (figure 3b). Consequently, the Euclidean path integral (3.13) can be expressed as [34]

$$K_+[\psi_L, \psi_R] = \langle \psi_R | e^{-\pi J} \Theta | \psi_L \rangle, \quad (3.26)$$

where we identify $\psi_1 = \psi_L$ and $\psi_2 = \psi_R$. Additionally, Θ is the anti-unitary CPT operator,

$$\Theta \phi_L \Theta^{-1} = \phi_R, \quad (3.27)$$

applied to the Rindler state in the left wedge, defined for $x < 0$ and evolving in t in reverse.

For the causal diamond, we use the mapping defined between the internal (external) region of the causal diamond and the right (left) Rindler wedge, given in (3.1). This allows

us to implement this transformation at the quantum level using the unitary operator

$$U = e^{-i(a^\alpha T_\alpha + b^\alpha K_\alpha)}, \quad (3.28)$$

where $b^\mu = (0, -\frac{1}{2\alpha})$ and $a^\mu = (0, -\alpha)$. Thus,

$$U\psi_R U^{-1} = \psi_{in}, \quad U\psi_L U^{-1} = \psi_{ext}. \quad (3.29)$$

Furthermore, from the action of the anti-unitary CPT operator Θ on the scalar fields in the left and right Rindler wedges, we obtain

$$\Theta_D = U\Theta U^{-1}, \quad (3.30)$$

from which we finally derive the anti-unitary operator Θ_D , which elaborates the map between the fields in the interior and exterior regions of the causal diamond,

$$\Theta_D \psi_{ext} \Theta_D^{-1} = \psi_{in}. \quad (3.31)$$

Applying (3.29) and (3.30) to (3.26), we have

$$\langle \psi_{in} | e^{-\pi J_D} \Theta_D | \psi_{ext} \rangle, \quad (3.32)$$

where $e^{-\pi J} \rightarrow e^{-\pi J_D} = U e^{-\pi J} U^{-1}$ is the conformal map that implements the rotation from the exterior region to the interior region of the causal diamond. This can be visualised by constructing the vector field $\partial_\tau = (\partial x^\mu / \partial \tau) \partial_\mu$ [35], taking into account the conformal transformation (3.2) (see figure 3c). In Euclidean signature, we have

$$\partial_\tau = \frac{1}{\alpha^2} \left(t_{E\bar{x}} \partial_x + \frac{1}{2} (\alpha^2 + t_E^2 - x^2) \partial_{t_E} \right). \quad (3.33)$$

Therefore, we observe that (3.33) maps the exterior region to the interior of the causal diamond through rotations of π (see figure 3d).

In conclusion, the identifications $\psi_1 = \psi_{ext}$ and $\psi_2 = \psi_{int}$ naturally emerge. Thus, the Euclidean path integral (3.13) represents the thermofield double state, describing the thermal nature of the “vacuum” with a temperature given by $T = \beta^{-1}$. In bra–ket notation notation, we have

$$|TFD\rangle = \frac{1}{\sqrt{Z(\beta)}} \sum_{n=0}^{\infty} e^{-\frac{\beta}{2} E_n} |n_{in}\rangle \otimes \Theta_D |n_{ext}\rangle. \quad (3.34)$$

4 Density matrix and Diamond Temperature

The Thermofield Double State (3.13) manifests itself as an entangled state of the ψ_1 and ψ_2 states. Here, ψ_2 is the fictitious field introduced by Umezawa and Takahashi, which in this analysis arises naturally when implementing the considerations made regarding Euclidean geometry. Consequently, the physical system under analysis will be described

by the reduced density matrix obtained by taking the partial trace of the total density matrix given by $\rho[\psi_1, \psi_2] = K_+[\psi_1, \psi_2]K_-[\psi_1, \psi_2]$. This is achieved by integrating out the fictitious field,

$$\rho[\psi_1] = \int_{-\infty}^{\infty} d\psi_2 \rho[\psi_1, \psi_2] = \frac{1}{Z(\beta)} \sum_{n=0}^{\infty} e^{-\beta E_n} \varphi_n(\psi_1) \varphi_n^*(\psi_1). \quad (4.1)$$

As we can observe, the perception of the observer's ground state in a causal diamond is determined by a thermal bath described by a canonical ensemble in thermal equilibrium at temperature β^{-1} .

Additionally, from the analysis of the cylinder's geometry (section 2.2), we know that β represents the period of the coordinate τ . Thus, it becomes essential to employ a coordinate transformation between the latter and the plane to establish the temperature associated with this periodicity within the framework of causal diamond geometry. Furthermore, in the context of this ongoing study, we will confine our analysis to the scenario where the observer is located at $x = 0$. In this manner, the transformations are delineated as follows

$$\tau(t_E, 0) = \alpha \tan^{-1} \left(\frac{2\alpha t_E}{\alpha^2 - t_E^2} \right), \quad \xi(t_E, 0) = 2\alpha. \quad (4.2)$$

This allows us to express the conformal factor in terms of t_E and α , which is given by $\Omega(t_E) = \frac{1}{2} \left(\frac{\alpha^2 + t_E^2}{2\alpha^2} \right)$. Consequently, by identifying the line elements of the Diamond and the plane, $\Omega(t_E)^2 \frac{(2\alpha)^2}{\alpha^2} dt^2 = dt_E^2$, it becomes possible to determine the value of β as perceived by the observer situated at $x = 0$, whose lifetime is limited to $t_E \in (-\alpha, \alpha)$. Thus,

$$\int_0^{\beta} d\tau = \int_{-\alpha}^{+\alpha} \frac{dt_E}{\left(\frac{\alpha^2 + t_E^2}{2\alpha^2} \right)} \quad \beta = \pi\alpha. \quad (4.3)$$

The temperature detected by the diamond observer is then given by $T = \beta^{-1} = (\pi\alpha)^{-1}$, which is exactly the diamond temperature found in the literature.

5 Conclusions

This article adds to a series of studies on the temperature of causal diamonds. The temperature perceived by a diamond observer has been obtained using the modular flow and thermal time hypothesis approach [18], Bogolyubov transformations [30], Unruh-deWitt detector formalism [28, 30], open quantum systems approach [31], among many others, and now, in this paper, using a path integral formalism. All these derivations lead to the same diamond temperature, which confirms the robustness of this result. It also corroborates the fact that the causal diamond thermality has all the characteristics of the Unruh effect even in the absence of acceleration, thus highlighting the fact that the study of causal diamonds demands more attention from the community. Recently, it has been established that conformal Killing vectors in the causal diamond geometry are closely related to the

generators of $sl(2, \mathbb{R})$ algebra in (0+1)-D conformal field theory, known as conformal quantum mechanics [23, 35–40]. On the other hand, conformal quantum mechanics plays an integral role in determining the temperature of black hole radiation [41–46], thus tying causal diamonds to the near-horizon physics of black holes more closely. Causal diamonds are also intriguing due to their connection with entanglement entropy in many-body systems and quantum chaos. These connections imply that causal diamonds can be the key to understanding the origin of black hole entropy and information scrambling in black holes. We intend to explore some of these topics in the future.

A Computation of the Euclidean Action

A.1 Massless field

Using the Fourier transformation for the real scalar field ϕ ,

$$\phi(\tau, \rho) = \frac{1}{2\pi} \int e^{i\rho\lambda} \phi(\tau, \lambda) d\lambda, \quad (\text{A.1})$$

in the action (3.8), we have

$$\begin{aligned} S_E &= -\frac{1}{2} \int d\rho d\tau \frac{1}{2\pi} \int e^{i\rho\lambda_1} \phi(\tau, \lambda_1) d\lambda_1 [\partial_\tau^2 + \partial_\rho^2] \frac{1}{2\pi} \int e^{-i\rho\lambda_2} \phi^*(\tau, \lambda_2) d\lambda_2 \\ &= -\frac{1}{2} \left(\frac{1}{2\pi} \right) \int d\tau d\lambda_1 d\lambda_2 \left[\frac{1}{2\pi} \int d\rho e^{i\rho(\lambda_1 - \lambda_2)} \right] \phi(\tau, \lambda_1) [\partial_\tau^2 - \lambda_2^2] \phi^*(\tau, \lambda_2) \\ &= -\frac{1}{2} \left(\frac{1}{2\pi} \right) \int d\tau d\lambda_1 d\lambda_2 \delta(\lambda_1 - \lambda_2) \phi(\tau, \lambda_1) [\partial_\tau^2 - \lambda_2^2] \phi^*(\tau, \lambda_2) \\ &= -\frac{1}{2} \int d\tau \left[\int \frac{d\lambda_1}{2\pi} \phi(\tau, \lambda_1) \partial_\tau^2 \phi^*(\tau, \lambda_1) - \int \frac{d\lambda_1}{2\pi} \phi(\tau, \lambda_1) \lambda_1^2 \phi^*(\tau, \lambda_1) \right]. \end{aligned}$$

Making the substitution $\phi = \sqrt{2\pi}\psi(\tau)\chi(\lambda)$ and requiring that $\psi(\tau)$ be real, consequently, $\chi(\lambda)$ will also be real, we obtain

$$S_E = -\frac{1}{2} \int d\tau \psi(\tau) \partial_\tau^2 \psi(\tau) \int d\lambda \chi(\lambda)^2 + \frac{1}{2} \int d\tau \psi(\tau)^2 \int d\lambda \lambda^2 \chi(\lambda)^2. \quad (\text{A.2})$$

Discretizing the integrals in λ , we have

$$\int d\lambda \chi(\lambda)^2 = \lim_{n \rightarrow \infty} \sum_{i=1}^n \chi(\lambda_i)^2 \Delta\lambda_i, \quad (\text{A.3})$$

$$\int d\lambda \lambda^2 \chi(\lambda)^2 = \lim_{n \rightarrow \infty} \sum_{i=1}^n \lambda_i^2 \chi(\lambda_i)^2 \Delta\lambda_i. \quad (\text{A.4})$$

Thus, the Euclidean action S_E for the mode $\lambda_k \rightarrow \lambda$, and setting $g(\lambda) = \chi(\lambda)^2 \Delta\lambda > 0$, is given by

$$S_E = -\frac{1}{2} \int d\tau [\psi(\tau) \partial_\tau^2 \psi(\tau) g(\lambda) - \psi(\tau)^2 \lambda^2 g(\lambda)].$$

Making the substitution $\psi_\lambda(\tau) = \psi(\tau) \sqrt{g(\lambda)}$, we have

$$S_E = -\frac{1}{2} \int d\tau \psi_\lambda(\tau) [\partial_\tau^2 - \lambda^2] \psi_\lambda(\tau). \quad (\text{A.5})$$

A.2 Massive field

The action (3.17) can be written as

$$S_E = I + II, \quad (\text{A.6})$$

where

$$I = -\frac{1}{2} \int d\xi d\tau \phi \left[\frac{\alpha}{\xi} \partial_\tau^2 + \frac{1}{\alpha \xi} A_\xi \right] \phi, \quad II = \frac{m^2}{2\alpha} \int d\xi d\tau \phi \left[\sum_{n=1} \xi^{n+1} f_n(\tau) \right] \phi.$$

Using $\phi(\tau, \xi) = \psi(\tau) \zeta(\xi) / \sqrt{\alpha}$ in II , we obtain

$$II = \sum_{n=1} \int d\tau f_n(\tau) \psi(\tau)^2 \int d\xi \frac{m^2}{2\alpha^2} \xi^{n+1} \zeta(\xi)^2. \quad (\text{A.7})$$

From the transformation (3.18), we have

$$\begin{aligned} II &= \sum_{n=1} \int d\tau f_n(\tau) \psi(\tau)^2 \int d\xi \frac{m^2}{2\alpha^2} \xi^{n+1} \int \frac{d\lambda_1}{\pi^2} \sinh(\pi\sqrt{\lambda_1}) K_{i\sqrt{\lambda_1}}(m\xi) \zeta(\lambda_1) \\ &\quad \times \int \frac{d\lambda_2}{\pi^2} \sinh(\pi\sqrt{\lambda_2}) K_{i\sqrt{\lambda_2}}(m\xi) \zeta(\lambda_2) \\ &= \frac{1}{2\alpha^2 \pi^4} \sum_{n=1} \int d\tau f_n(\tau) \psi(\tau)^2 \int d\lambda_1 \sinh(\pi\sqrt{\lambda_1}) \zeta(\lambda_1) \\ &\quad \times \int d\lambda_2 \sinh(\pi\sqrt{\lambda_2}) \zeta(\lambda_2) II_\xi^n, \end{aligned}$$

where II_ξ is the integral over ξ , and its solution is

$$\begin{aligned} II_\xi^n &= \int d\xi m^2 \xi^{n+1} K_{i\sqrt{\lambda_1}}(m\xi) K_{i\sqrt{\lambda_2}}(m\xi) \\ &= \frac{m^{-n} 2^{n-1}}{\Gamma[n+2]} \Gamma\left[\frac{1}{2} (n + i\sqrt{\lambda_1} + i\sqrt{\lambda_2} + 2)\right] \Gamma\left[\frac{1}{2} (n - i\sqrt{\lambda_1} - i\sqrt{\lambda_2} + 2)\right] \\ &\quad \times \Gamma\left[\frac{1}{2} (n + i\sqrt{\lambda_1} - i\sqrt{\lambda_2} + 2)\right] \Gamma\left[\frac{1}{2} (n - i\sqrt{\lambda_1} + i\sqrt{\lambda_2} + 2)\right]. \end{aligned} \quad (\text{A.8})$$

We note that for $m \gg 1$, the integral II_ξ^n goes to zero for each value of n . Therefore, it becomes possible to neglect the integral II in the action (A.6). Consequently,

$$S_E = -\frac{1}{2} \int d\tau \psi(\tau) \partial_\tau^2 \psi(\tau) \int \frac{d\xi}{\xi} \zeta(\xi)^2 - \frac{1}{2\alpha^2} \int d\tau \psi(\tau)^2 \int \frac{d\xi}{\xi} \zeta(\xi) A_\xi \zeta(\xi). \quad (\text{A.9})$$

Applying the transformation (3.18) and the differential equation $A_\xi K_{i\sqrt{\lambda}}(m\xi) = -\lambda K_{i\sqrt{\lambda}}(m\xi)$, we have

$$\begin{aligned} S_E &= -\frac{1}{2} \int d\tau \psi(\tau) \partial_\tau^2 \psi(\tau) \int \frac{d\lambda}{\pi^2} \zeta(\lambda) \sinh(\pi\sqrt{\lambda}) \int d\xi \frac{\zeta(\xi)}{\xi} K_{i\sqrt{\lambda}}(m\xi) \\ &\quad + \frac{1}{2\alpha^2} \int d\tau \psi(\tau)^2 \int \frac{d\lambda}{\pi^2} \lambda \zeta(\lambda) \sinh(\pi\sqrt{\lambda}) \int d\xi \frac{\zeta(\xi)}{\xi} K_{i\sqrt{\lambda}}(m\xi). \end{aligned}$$

From the transformation (3.19), we obtain

$$S_E = -\frac{1}{2} \int d\tau \psi(\tau) \partial_\tau^2 \psi(\tau) \int \frac{d\lambda}{\pi^2} \zeta(\lambda)^2 \sinh(\pi\sqrt{\lambda}) + \frac{1}{2\alpha^2} \int d\tau \psi(\tau)^2 \int \frac{d\lambda}{\pi^2} \lambda \zeta(\lambda)^2 \sinh(\pi\sqrt{\lambda}).$$

Discretizing the integrals in λ , we have

$$\int \frac{d\lambda}{\pi^2} \zeta(\lambda)^2 \sinh(\pi\sqrt{\lambda}) = \lim_{n \rightarrow \infty} \sum_{i=1}^n g(\lambda_i), \quad (\text{A.10})$$

$$\int \frac{d\lambda}{\pi^2} \lambda \zeta(\lambda)^2 \sinh(\pi\sqrt{\lambda}) = \lim_{n \rightarrow \infty} \sum_{i=1}^n \lambda_i g(\lambda_i). \quad (\text{A.11})$$

where $g(\lambda_i) = \frac{1}{\pi^2} \zeta(\lambda_i)^2 \sinh(\pi\sqrt{\lambda_i}) \Delta \lambda_i > 0$. So, the Euclidean action S_E for each mode $\lambda_k \rightarrow \lambda$ is given by

$$S_E = -\frac{1}{2} \int d\tau \left[\psi(\tau) \partial_\tau^2 \psi(\tau) g(\lambda) - \psi(\tau)^2 \frac{\lambda}{\alpha^2} g(\lambda) \right].$$

Making the substitutions $\psi_\lambda(\tau) = \psi(\tau) \sqrt{g(\lambda)}$ and $\lambda/\alpha^2 = \omega_\lambda^2$, we obtain

$$S_E = -\frac{1}{2} \int d\tau \psi_\lambda(\tau) [\partial_\tau^2 - \omega_\lambda^2] \psi_\lambda(\tau). \quad (\text{A.12})$$

Acknowledgments

CRO was partially supported by the Army Research Office (ARO), Grant W911NF-23-1-0202.

References

- [1] S.W. Hawking, *Black hole explosions*, *Nature* **248** (1974) 30.
- [2] S.W. Hawking, *Particle Creation by Black Holes*, *Commun. Math. Phys.* **43** (1975) 199.
- [3] S.W. Hawking, *Black Holes and Thermodynamics*, *Phys. Rev. D* **13** (1976) 191.
- [4] W.G. Unruh, *Notes on black hole evaporation*, *Phys. Rev. D* **14** (1976) 870.
- [5] P.C.W. Davies, S.A. Fulling and W.G. Unruh, *Energy Momentum Tensor Near an Evaporating Black Hole*, *Phys. Rev. D* **13** (1976) 2720.
- [6] P.C.W. Davies and S.A. Fulling, *Radiation from a moving mirror in two-dimensional space-time conformal anomaly*, *Proc. Roy. Soc. Lond. A* **348** (1976) 393.
- [7] P.C.W. Davies, *Thermodynamics of Black Holes*, *Proc. Roy. Soc. Lond. A* **353** (1977) 499.
- [8] P.C.W. Davies, *Scalar particle production in Schwarzschild and Rindler metrics*, *J. Phys. A* **8** (1975) 609.
- [9] R.M. Wald, *On Particle Creation by Black Holes*, *Commun. Math. Phys.* **45** (1975) 9.

- [10] L. Parker, *Probability Distribution of Particles Created by a Black Hole*, *Phys. Rev. D* **12** (1975) 1519.
- [11] Y. Takahashi and H. Umezawa, *Thermo field dynamics*, *Collect. Phenom.* **2** (1975) 55.
- [12] H. Umezawa, H. Matsumoto and M. Tachiki, *THERMO FIELD DYNAMICS AND CONDENSED STATES* (1982).
- [13] H. Matsumoto, Y. Nakano, H. Umezawa, F. Mancini and M. Marinaro, *Thermo Field Dynamics in Interaction Representation*, *Prog. Theor. Phys.* **70** (1983) 599.
- [14] Y. Takahashi and H. Umezawa, *Thermo field dynamics*, *Int. J. Mod. Phys. B* **10** (1996) 1755.
- [15] W. Israel, *Thermo field dynamics of black holes*, *Phys. Lett. A* **57** (1976) 107.
- [16] R. Laflamme, *THERMO FIELDS FROM EUCLIDEAN PATH INTEGRALS*, *Physica A* **158** (1989) 58.
- [17] R. Laflamme, *Geometry and Thermofields*, *Nucl. Phys. B* **324** (1989) 233.
- [18] P. Martinetti and C. Rovelli, *Diamonds's temperature: Unruh effect for bounded trajectories and thermal time hypothesis*, *Class. Quant. Grav.* **20** (2003) 4919 [[gr-qc/0212074](#)].
- [19] P. Martinetti, *Conformal mapping of Unruh temperature*, *Mod. Phys. Lett. A* **24** (2009) 1473 [[0803.1538](#)].
- [20] T. Jacobson and M. Visser, *Gravitational Thermodynamics of Causal Diamonds in (A)dS*, *SciPost Phys.* **7** (2019) 079 [[1812.01596](#)].
- [21] T. Jacobson and M.R. Visser, *Entropy of causal diamond ensembles*, *SciPost Phys.* **15** (2023) 023 [[2212.10608](#)].
- [22] J. Wang, *Geometry of small causal diamonds*, *Phys. Rev. D* **100** (2019) 064020 [[1904.01034](#)].
- [23] M. Arzano, *Conformal quantum mechanics of causal diamonds*, *JHEP* **05** (2020) 072 [[2002.01836](#)].
- [24] T. Banks, *Emergence of Quantum Field Theory in Causal Diamonds*, .
- [25] V. Chandrasekaran and K. Prabhu, *Symmetries, charges and conservation laws at causal diamonds in general relativity*, *JHEP* **10** (2019) 229 [[1908.00017](#)].
- [26] J. de Boer, F.M. Haehl, M.P. Heller and R.C. Myers, *Entanglement, holography and causal diamonds*, *JHEP* **08** (2016) 162 [[1606.03307](#)].
- [27] G.W. Gibbons and S.N. Solodukhin, *The Geometry of small causal diamonds*, *Phys. Lett. B* **649** (2007) 317 [[hep-th/0703098](#)].
- [28] J. Foo, S. Onoe, M. Zych and T.C. Ralph, *Generating multi-partite entanglement from the quantum vacuum with a finite-lifetime mirror*, *New J. Phys.* **22** (2020) 083075 [[2004.07094](#)].
- [29] R. Andrade e Silva and T. Jacobson, *Causal diamonds in (2+1)-dimensional quantum gravity*, *Phys. Rev. D* **107** (2023) 024033 [[2203.10084](#)].
- [30] D. Su and T.C. Ralph, *Spacetime diamonds*, *Phys. Rev. D* **93** (2016) 044023 [[1507.00423](#)].
- [31] A. Chakraborty, H. Camblong and C. Ordonez, *Thermal effect in a causal diamond: Open quantum systems approach*, *Phys. Rev. D* **106** (2022) 045027 [[2207.08086](#)].
- [32] M. Kontorovich and N. Lebedev, *On the one method of solution for some problems in diffraction theory and related problems*, *J. Exp. Theor. Phys.* **8** (1938) 1192.
- [33] N. Lebedev, *Sur une formule d'inversion*, *CR Acad. Sci. URSS* **52** (1946) 302.

- [34] D. Harlow, *Jerusalem Lectures on Black Holes and Quantum Information*, *Rev. Mod. Phys.* **88** (2016) 015002 [[1409.1231](#)].
- [35] T. Jacobson, *Entanglement Equilibrium and the Einstein Equation*, *Phys. Rev. Lett.* **116** (2016) 201101 [[1505.04753](#)].
- [36] M. Arzano, *Vacuum thermal effects in flat space-time from conformal quantum mechanics*, *JHEP* **07** (2021) 003 [[2103.07228](#)].
- [37] M. Arzano, A. D’Alise and D. Frattulillo, *Entanglement entropy in conformal quantum mechanics*, *JHEP* **10** (2023) 165 [[2306.12291](#)].
- [38] T. De Lorenzo and A. Perez, *Light Cone Thermodynamics*, *Phys. Rev. D* **97** (2018) 044052 [[1707.00479](#)].
- [39] T. De Lorenzo and A. Perez, *Light Cone Black Holes*, *Phys. Rev. D* **99** (2019) 065009 [[1811.03667](#)].
- [40] A. Herrero and J.A. Morales, *Radial conformal motions in minkowski space-time*, *Journal of Mathematical Physics* **40** (1999) 3499.
- [41] H.E. Camblong and C.R. Ordóñez, *Black hole thermodynamics from near-horizon conformal quantum mechanics*, *Phys. Rev. D* **71** (2005) 104029 [[hep-th/0411008](#)].
- [42] H.E. Camblong and C.R. Ordóñez, *Semiclassical methods in curved spacetime and black hole thermodynamics*, *Phys. Rev. D* **71** (2005) 124040 [[hep-th/0412309](#)].
- [43] H.E. Camblong, A. Chakraborty and C.R. Ordóñez, *Near-horizon aspects of acceleration radiation by free fall of an atom into a black hole*, *Phys. Rev. D* **102** (2020) 085010 [[2009.06580](#)].
- [44] A. Azizi, H.E. Camblong, A. Chakraborty, C.R. Ordóñez and M.O. Scully, *Acceleration radiation of an atom freely falling into a Kerr black hole and near-horizon conformal quantum mechanics*, *Phys. Rev. D* **104** (2021) 065006 [[2011.08368](#)].
- [45] A. Azizi, H.E. Camblong, A. Chakraborty, C.R. Ordóñez and M.O. Scully, *Quantum optics meets black hole thermodynamics via conformal quantum mechanics: I. Master equation for acceleration radiation*, *Phys. Rev. D* **104** (2021) [[2108.07570](#)].
- [46] A. Azizi, H.E. Camblong, A. Chakraborty, C.R. Ordóñez and M.O. Scully, *Quantum optics meets black hole thermodynamics via conformal quantum mechanics: II. Thermodynamics of acceleration radiation*, *Phys. Rev. D* **104** (2021) [[2108.07572](#)].